International Journal of Nanomedicine

Dovepress
open access to scientific and medical research

Open Access Full Text Article

ORIGINAL RESEARCH

Alzheimer's Disease Determination by a Dual Probe on Gold Nanourchins and Nanohorn Hybrids

This article was published in the following Dove Press journal:
International Journal of Nanomedicine

Zhengguo Qiu,[1] Qianhe Shen,[2] Chao Jiang,[3] Li Yao,[4] Xiaopeng Sun,[5] Jing Li,[6] Chongzhen Duan,[1] Rui Li,[1] Xiuli Li,[1] Subash CB Gopinath,[7,8] Periasamy Anbu,[9] Thangavel Lakshmipriya,[8] Xu Li[10]

[1]Department of Anesthesiology, Affiliated Hospital of Shaanxi University of Traditional Chinese Medicine, Xianyang, Shaanxi, 712000, People's Republic of China; [2]Department of Anesthesiology, Xi'an GemFlower Changqing Hospital, Xi'an, Shaanxi, 710200, People's Republic of China; [3]The Third Department of Neurology, The Second Affiliated Hospital of Xi'an Medical University, Xi'an, Shaanxi, 710038, People's Republic of China; [4]Department of Neurology, The Hospital of Xidian Group, Xi'an, Shaanxi, 710077, People's Republic of China; [5]Department of Otolaryngology, The Second Affiliated Hospital of Xi'an Medical University, Xi'an, Shaanxi, 710038, People's Republic of China; [6]Department of Anesthesiology, The Second Affiliated Hospital of Xi'an Medical University, Xi'an, Shaanxi, 710038, People's Republic of China; [7]Faculty of Chemical Engineering Technology, Universiti Malaysia Perlis (UniMAP), Arau, Perlis, 02600, Malaysia; [8]Institute of Nano Electronic Engineering, Universiti Malaysia Perlis (UniMAP), Kangar, 01000, Malaysia; [9]Department of Biological Engineering, College of Engineering, Inha University, Incheon, 402-751, Republic of Korea; [10]Department of Surgery and Anesthesiology, Xi'an Hospital of Traditional Chinese Medicine, Xi'an, Shaanxi, People's Republic of China

Correspondence: Xu Li
Email qzg2020@sina.com

Background: Alzheimer's disease (AD) is a neurodegenerative chronic disorder that causes dementia and problems in thinking, cognitive impairment and behavioral changes. Amyloid-beta (Aβ) is a peptide involved in AD progression, and a high level of Aβ is highly correlated with severe AD. Identifying and quantifying Aβ levels helps in the early treatment of AD and reduces the factors associated with AD.

Materials and Methods: This research introduced a dual probe detection system involving aptamers and antibodies to identify Aβ. Aptamers and antibodies were attached to the gold (Au) urchin and hybrid on the carbon nanohorn-modified surface. The nanohorn was immobilized on the sensor surface by using an amine linker, and then a Au urchin dual probe was immobilized.

Results: This dual probe-modified surface enhanced the current flow during Aβ detection compared with the surface with antibody as the probe. This dual probe interacted with higher numbers of Aβ peptides and reached the detection limit at 10 fM with R^2=0.992. Furthermore, control experiments with nonimmune antibodies, complementary aptamer sequences and control proteins did not display the current responses, indicating the specific detection of Aβ.

Conclusion: Aβ-spiked artificial cerebrospinal fluid showed a similar response to current changes, confirming the selective identification of Aβ.

Keywords: amyloid-beta, biomarker, nanomaterial, aptamer, antibody

Introduction

Alzheimer's disease (AD) is a chronic neurodegenerative disorder affecting older people that causes cognitive impairment, memory loss, changing personality and dementia. AD is irreversible and is becoming a serious health concern worldwide, with more than thirty-five million people affected.[1,2] Behavioral and personality changes and the degree of memory loss are the first indications of AD. Brain imaging tests with magnetic resonance analysis, and computerized tomography have been utilized to identify AD.[3] Recently, positron emission tomography (PET) was used to identify specific regions of the brain with decreased glucose metabolism, which helps to distinguish different brain degenerative diseases. Additionally, PET scans were used to identify cluster formation by amyloid plaques, which is closely associated with dementia caused by AD. However, these types of identification methods are expensive and uncomfortable for older people. Therefore, identification by blood-based biomarkers is an alternative way to diagnose AD, making it cost-effective and convenient.[4,5] Moreover, various biomarkers, such as microRNAs, proteins, peptides, antibodies and receptors, can

identify AD and help to treat AD in its earlier stages.[2,4,6] Since the condition caused by AD is irreversible, early detection of AD helps to establish a routine life for patients.

Aggregation and misfolding of amyloid-beta (Aβ) is a potential mechanism in AD patients.[7] Aβ monomers assemble into AβO (Aβ oligomers) and fibrils and are then distributed into the circulating blood or cerebrospinal fluid (CSF).[1] The AβO is neurotoxic and is highly correlated with severe AD. Various studies have confirmed that the AβO concentration is much higher in AD patients than in normal patients.[1,8] Moreover, the AβO level in CSF helps to predict the progression at earlier and periclinal stages of AD. Therefore, using AβO as a biomarker is not only useful for identification but also helps as a therapeutic target for AD.[9] Various sensors, such as surface plasmon resonance, electrochemical sensors, enzyme-linked immunosorbent assays, RAMAN spectroscopy and fluorescent sensors, have been utilized to measure AβO with the help of proteins, peptides, and antibodies.[8,10–13] However, it is still challenging to identify AβO with high specificity in biological fluids without nonspecific adsorption and interference. This research involved design of a combined dual probe with an aptamer and antibody on the surface of a gold (Au) urchin to identify AβO on a triangular electrochemical sensor.

Probe selection and immobilization on the sensor surface play a major role in achieving lower-level detection of the target molecule. There are various kinds of probes, such as RNA, DNA, aptamers, antibodies, peptides and enzymes, commonly used to detect analyte molecules.[14] Among these, antibodies are more attractive and promising probes for the detection of biomolecules due to their selectivity and higher affinities for their targets. Due to the selectivity, an antibody was also used to detect the analyte even in a crude sample. On the other hand, aptamers are artificial antibodies that perform similar roles as antibodies in many biological applications. They can be artificially generated by the SELEX (systematic evaluation of ligands and exponential enrichment) process with the three simple steps of binding, separation and amplification.[15–17] Even though aptamers are widely applied in biological fields, work has been highly focused on developing biosensors due to the high specificity and selectivity of aptamers with their targets. Various aptamers have been generated for a wide range of targets for diagnosis and therapeutic purposes.[18,19] In particular, aptamers and antibodies were used to implement sandwich assays to identify the target at a lower level and this indicate that sandwich assays with aptamers and antibodies displayed high performance levels.[20,21] In most cases, an aptamer was used as the capture probe due to its strong binding to the target, and an antibody was used as the detection probe. However, this method of detection requires many steps and is time consuming. Therefore, this study introduces a dual probe consisting of an aptamer and antibody on an independent Au urchin surface to identify AβO. This probe was attached to the nanoform-decorated triangular sensor, and AβO was detected at a lower level relative to a single platform.

Carbon nanohorns (CNHs) are carbon-based materials that have recently attracted considerable attention for various applications in different fields, where they are used in solar thermal collectors, supercapacitors, and fuel cells, and for photovoltaic and biomedical applications.[22,23] In particular, CNHs are attractive in the biosensing field due to their high dispersibilities, high conductivities and large surface areas. Since CHNs improve the mechanical and electrical properties, researchers were encouraged to apply them in electrochemical sensors.[24,25] Apart from that, the surface modification of CNHs is easily accomplished through the conical ends of CNHs with thiols, amines, and different types of pyrene and porphyrin derivatives.[22] In the current research, a CNH was decorated onto a sensing surface to improve current flow and utilized to attach a dual probe (aptamer and antibody) to a Au urchin and identify AβO. The CNH was immobilized on the electrode surface by using the amine (3-aminopropyl)triethoxysilane (APTMS) linker, and then the dual probe was attached on the nanohorn through the amine on the APTMS with the Au urchin. This dual probe-attached surface was utilized to identify AβO for the diagnosis of AD.

Materials and Methods

Reagents and Biomolecules

Ethanolamine, gold urchin, nanohorn, 16-mercaptoundecanoic acid, 3-(3-dimethylaminopropyl)carbodiimide (EDC), N-hydroxysulfosuccinimide (sulfo-NHS) and APTMS were received from Sigma Aldrich (USA). Aβ (1–42) was purchased from DgPeptides Co., Ltd, China. Anti- Aβ antibody was obtained from Abcam (England). The aptamer sequence (5′-SH-GCCTGTGTTGGGGCGGGTGCG) was reported by Tsukakoshi et al and synthesized commercially (Apical Scientific, Malaysia).[26] Artificial CSF was prepared by mixing

3.0 mM KCl, 150 mM NaCl, 0.8 mM $MgCl_2 \cdot 6H_2O$, 1 mM phosphate and 1.4 mM $CaCl_2 \cdot 2H_2O$.[27,28]

Morphological Imaging of Au Urchin and Nanohorn

Morphological images of the Au urchin, nanohorn and Au urchin-nanohorn hybrid were analyzed by field emission scanning electron microscopy (FESEM), field emission transmission electron microscopy (FETEM) and atomic force microscopy (AFM) or scanning AFM. Further energy dispersive X-ray (EDX) analysis was also conducted to confirm the elemental composition of the nanohorn and Au urchin.

Preparation of Anti-Aβ Antibody Conjugation with Au Urchin

Anti-Aβ antibody was conjugated on the surface of the Au urchin through 16-mercaptoundecanoic acid and EDC-NHS linker. Briefly, 500 µL of Au urchin was mixed with 16-mercaptoundecanoic acid (16-MDA, 5 mM) and kept for 1 hour at RT. After that, the unbound 16-MDA was separated by centrifugation. Subsequently, 16-MDA-linked Au urchin was activated by EDC and NHS (1:1) at 1 mM and stirred at room temperature for 10 min, and then the unbound EDC-NHS was removed by centrifugation. Finally, 10 µL of 250 nM anti-Aβ antibody was added to the Au urchin mixture and stirred continuously for 2 hours. The unbound antibodies were separated by centrifugation (8000 rpm for 10 min) followed by washing with distilled water three times to remove the unbound antibodies completely. The final antibody-Au urchin product was kept at 4 °C for further experiments.

Preparation and Optimization of Dual Probes of Aβ Antibodies and Aptamer-Conjugated Au Urchins

To prepare a dual probe of aptamer and antibody on a Au urchin, the Au urchin antibody was first prepared as explained previously. After that, thiolated Aβ aptamer was added to this solution (final concentration of 100 pM) and kept at RT for 1 hr to immobilize the aptamer on the remaining surface of the Au urchin. After that, the conjugated Au urchin-antibody-aptamer probe was separated by centrifugation and with three washings with distilled water. The same experiment was conducted with different aptamer concentrations (1 nM, 10 nM, 100 nM and 1 µM).

Multiple Junction Triangle Dielectrode (MJTD) Fabrication

Multiple junction triangle electrodes were fabricated with the traditional wet-etching procedure. First, the electrode pattern was designed by AutoCAD software.[29,30] The sensor surface was organized by two electrodes with multiple junction triangles at equal micro gap distances. The following steps were used to prepare the electrode. (i) A silicon wafer substrate was thermally oxidized at 500°C to form a silicon dioxide (SiO_2) layer; (ii) Aluminum was coated using a thermal evaporator; (iii) a 2000 nm thick layer of positive photoresist was applied by a spin-coater and then soft-baked at 90°C for 1 h; (iv) UV-light exposure was carried out for 10 s to transform the desired pattern on the photoresist; (v) the electrode was dipped in the developing solution to remove the desired area and then subjected to hard-baking at 110°C for 1 min; (vi) the electrode was immersed in Al-etching solution and then washed with distilled water and acetone. The final product was kept in a dry place for further experiments.

Aβ Oligomer (AβO) Preparation

To obtain the Aβ monomer, an Aβ solution with a concentration of 2 mg/mL was suspended in 1 mg/mL 100% HFIP (1,1,1,3,3,3-hexafluoroisopropanol) and this mixture was incubated overnight at room temperature under shaking conditions. HFIP worked as a hydrogen bond breaker to remove the pre-existing structural inhomogeneity of Aβ. The next day, the HFIP solvent was evaporated by treating the mixture under N_2 gas. Then, HFIP-treated Aβ was suspended in 100 µL of 1 mM NaOH and diluted to 100 µM in PBS buffer to obtain the monomer. Further, the Aβ monomer was kept at 37 °C overnight to form the Aβ oligomer (AβO), and then the formed AβO was separated from the insoluble aggregates by centrifugation at 10,000 x g for 15 min. All the prepared solutions were aliquoted immediately and stored at −20 °C for further use.

Detection of AβO by Antibody or Antibody-Aptamer or a Dual Probe of Aptamer and Antibody

AβO was detected on the MJTD surface and the following three methods were compared.

Detection of AβO by Au Urchin-Antibody

In this method, an anti-Aβ antibody-modified Au urchin was attached to the sensing electrode surface through the APTMS linker. First, the surface was treated with 1% KOH for 10 min, and then APTMS-nanohorn was added and incubated for 3 h. After washing the surface with ethanol (30%), antibody-Au urchin was added and incubated for 1 h. Then, the electrode was washed three times with PBS to eliminate the unbound aptamer. After that, the excess sensing electrode was covered with 1 mg/mL diluted PEG-NH_2. Different concentrations of AβO were allowed to interact with the immobilized antibody. The current response was noted before and after each immobilization process.

Detection of AβO by Au Urchin-Antibody Aptamer (Two Step)

In this method, AβO was detected by an aptamer and antibody with a two-step process. The following steps were involved in this detection strategy: (i) the surface was modified with APTMS nanohorns; (ii) Au urchin antibody was immobilized on the APTMS nanohorns; (iii) the remaining areas were blocked with 1 mg/mL diluted PEG-NH_2; (iv) different concentrations of aptamer were added; and (v) different concentrations of AβO were added to determine the limit of detection.

Detection of AβO by Au Urchin-Antibody Aptamer (Single Step)

In this method, AβO was detected by aptamer and antibody with a single step attachment. The following steps were involved in this detection strategy: (i) the surface was modified with APTMS nanohorns; (ii) the Au urchin antibody was immobilized on APTMS nanohorns; (iii) the remaining areas were blocked with 1 mg/mL diluted PEG-NH_2; (iv) a dual probe of antibody-aptamer was added; and (v) different concentrations of AβO were added to determine the limit of detection.

Selective Detection of AβO

To identify specific AβO detection, the following control experiments were conducted. The experiments were performed (i) without AβO; (ii) with nonimmune antibody and complementary aptamer sequence; and (iii) with α-synuclein instead of AβO. The current responses in control experiments were compared with those for the specific AβO detection. To determine the detection of AβO in a real-life sample, different AβO concentrations (0.01, 0.1, 1 and 10 pM) were spiked in artificial CSF and dripped on a dual probe immobilized surface. The other experimental setup was used as described above.

Results and Discussion

Figure 1 shows a schematic diagram for AβO determination on a nanohorn-modified dielectrode surface. Three different probe surfaces are compared to identify AβO, which includes only Au-urchin conjugated antibody, antibody-aptamer (two-steps) and a dual probe with antibody and aptamer (single step). In the first experiment, a Au-urchin antibody was attached to the nanohorn-modified surface through an APTMS linker. APTMS-modified nanohorns were attached to the dielectrode by reacting the amine on the nanohorn and the OH on the electrode surface. Then, the Au-antibody was conjugated onto the electrode through the electrostatic interactions of amine on the nanohorn with the Au surface or amine on the nanohorn with COOH on the antibody. AβO was detected on these antibody-modified surfaces. In the second experiment, using the same method, Au-urchin antibody was immobilized first. Then, an aptamer was added until the saturation point was attained. This thiol-linked aptamer bound to the remaining gold surface and was used to detect AβO. In the last experiment, before the immobilization of the Au urchin antibody, the aptamer was attached to the remaining Au urchin (aptamer and antibody on Au-urchin) and then immobilized on a nanohorn-modified surface. AβO detection on this surface was compared with the above two methods.

Characterization of Nanohorn and Nanohorn-Au Urchin with FESEM and EDX

The surface structure of the Au urchin was initially analyzed by AFM and FETEM. Figure 2A shows AFM observations of an intact particle with uniformity. The surface scan of the Au urchin clearly displayed the expected size of approximately 55 nm (Figure 2B). Figure 2C is the FETEM image of the Au urchin, distributed uniformly with an urchin shape. The EDX result confirmed the presence of Au at a 65% level (Figure 2D and E). Furthermore, the morphologies of Au-urchin, nanohorn and antibody-Au urchin immobilized on the sensing electrode were observed by FESEM analysis.

Figure 3A and B shows the FESEM image of the Au urchin, which is uniformly displayed in the 3D shape of urchin, and the related EDX confirmed the presence of

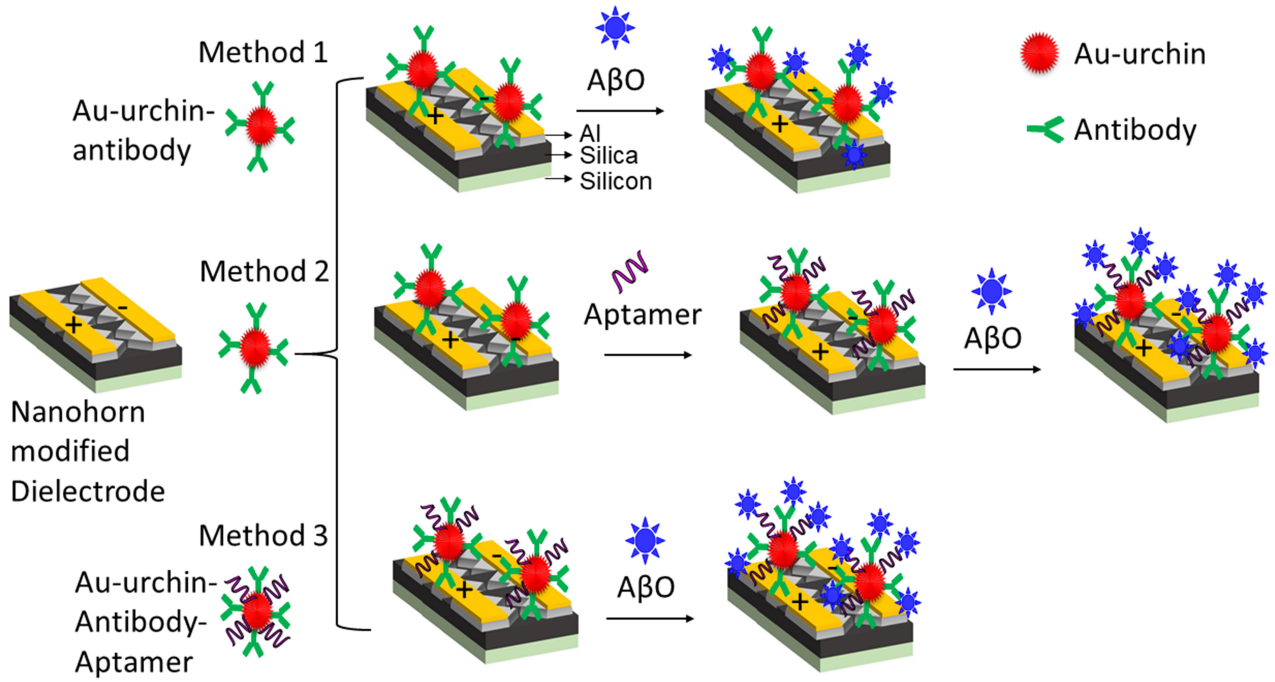

Figure 1 Schematic illustration of AβO determination on a nanohorn-modified dielectrode. Three methods of AβO detection were compared with the probes of (i) Au-urchin antibody; (ii) Au-urchin antibody-aptamer; and (iii) dual probe of aptamer and antibody on Au urchin.

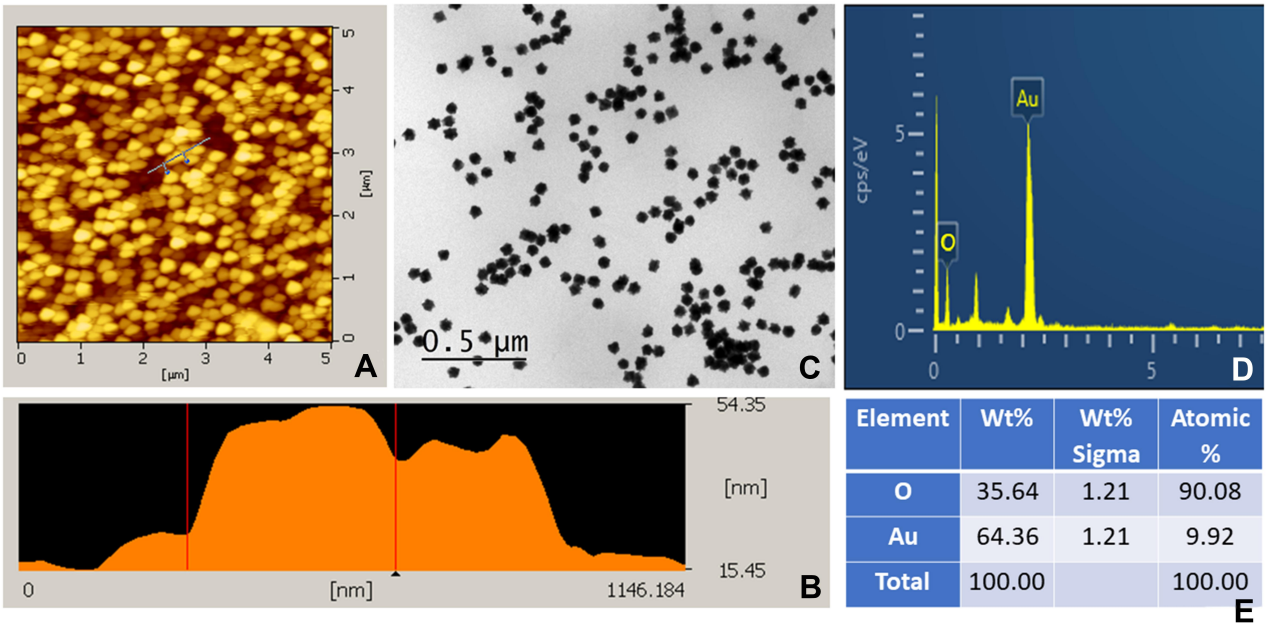

Element	Wt%	Wt% Sigma	Atomic %
O	35.64	1.21	90.08
Au	64.36	1.21	9.92
Total	100.00		100.00

E

Figure 2 Surface analysis by EDX. (**A**) AFM image of Au urchin; (**B**) surface of Au urchin-attached wafer; (**C**) FETEM image of Au urchin; (**D**) EDX analysis of Au urchin; (**E**) elemental composition of Au urchin. EDX results confirm the presence of carbon and gold on the immobilized surface.

100% gold. Figure 3C and D insets are FESEM images of the nanohorn, displaying a circular shape of the horn on the surface with a uniform distribution. The EDX result for the nanohorn showed that the major elements were C at 89% and O at 5.9%. Figure 3E and F displays the FESEM image of the antibody-Au-urchin conjugated nanohorn immobilized on the electrode surface. The figure shows a Au urchin similar to the nanohorn, but a spike on the nanohorn was

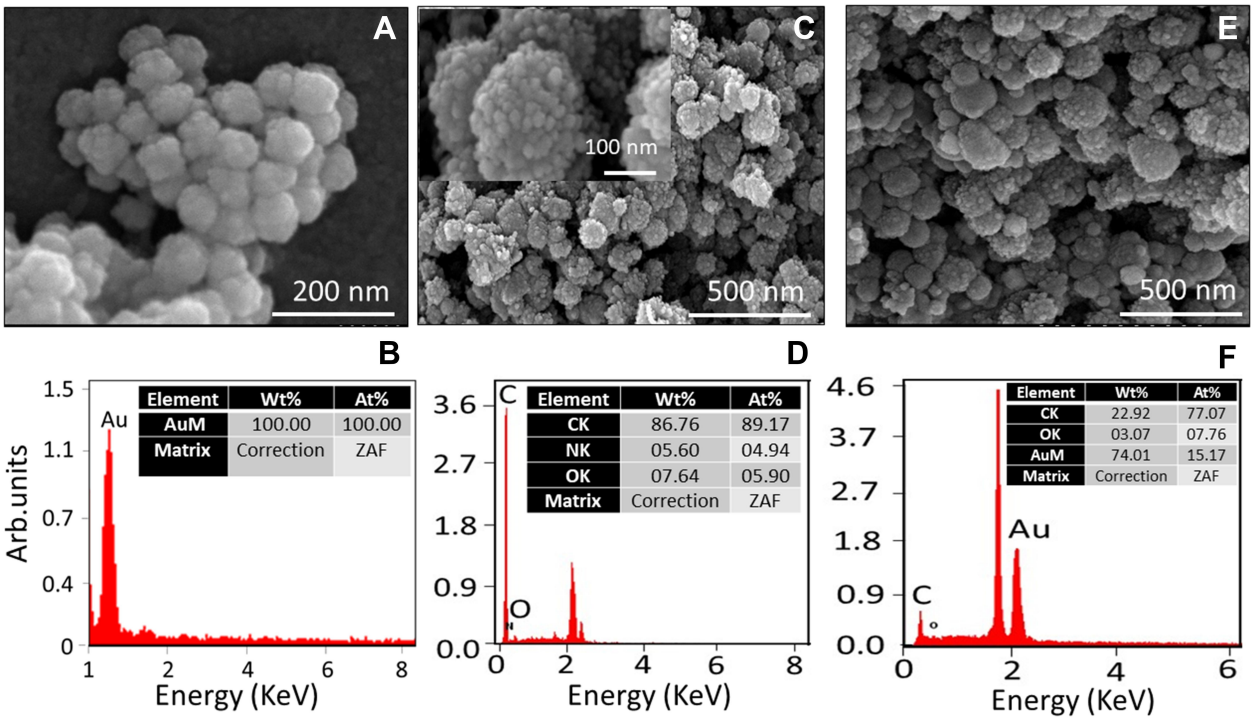

Figure 3 Surface morphology of the nanomaterial-modified electrode. (**A**) FESEM image of Au urchin; (**B**) EDX analysis of Au urchin; (**C**) FESEM image of nanohorn; Figure inset is at higher magnification. (**D**) EDX analysis of nanohorns; (**E**) FESEM image of Au-urchin antibody on nanohorns; (**F**) EDX analysis of Au-urchin antibody on nanohorns. EDX results confirm the presence of carbon and gold on the immobilized surfaces.

noticeable. Furthermore, the EDX results confirmed the presence of 77% C and 15% Au. This result confirms the binding of antibody-conjugated Au-urchin on the electrode surface. This electrode surface was utilized to determine AβO.

Probe Immobilization on a Nanohorn-Modified Dielectrode Surface: Target Interaction

Three different methods of probe immobilization, antibody, antibody-aptamer and antibody, and aptamer as a dual probe on Au urchin, were compared for efficient detection of AβO. Figure 4A displays the current response of antibody immobilization on the nanohorn-modified electrode. With each step, the current response was recorded to confirm the immobilization process. The KOH-treated bare dielectrode showed a current level of 5 E-07 A. After modifying the surface with the APTMS nanohorn, the surface current was increased to 1.24E-05 A. Furthermore, when the Au urchin antibody was added, the current response was increased to 3.57E-05 A. This increase in current occurred due to the interaction of APTMS on the nanohorns with COOH in the antibody and Au urchin with the APTMS molecule. In general, APTMS is a potential linker to attach antibodies to the sensing surfaces. Proper orientation of the antibody attachment on APTMS enhances the performance of the sensor. A nanohorn was utilized here to attach a higher number of APTMS molecules on the electrode, which automatically increased the number of attached antibodies on the electrode surface. In addition, the nanohorn improved the electrical flow upon binding biomolecules on the sensing surface. Apart from that, on the surface of the Au urchin, a higher number of antibodies was attached, which also enhanced antibody attachment on the electrode surface. After the surface was modified by antibody, the excess APTMS surface was covered with PEG-NH_2. APTMS attracts other biomolecules through electrostatic interactions, which leads to false positive detection of AβO. Therefore, it is mandatory to cover the excess APTMS; here, PEG polymer was used as the blocking agent. Various studies have proven that surface modification with PEG polymers gives a proper arrangement of biomolecules on sensing surfaces and reduces the signal-to-noise ratio.[20,31,32] This antibody-modified surface (method 1) was used to compare the detection of AβO with those of other methods described below.

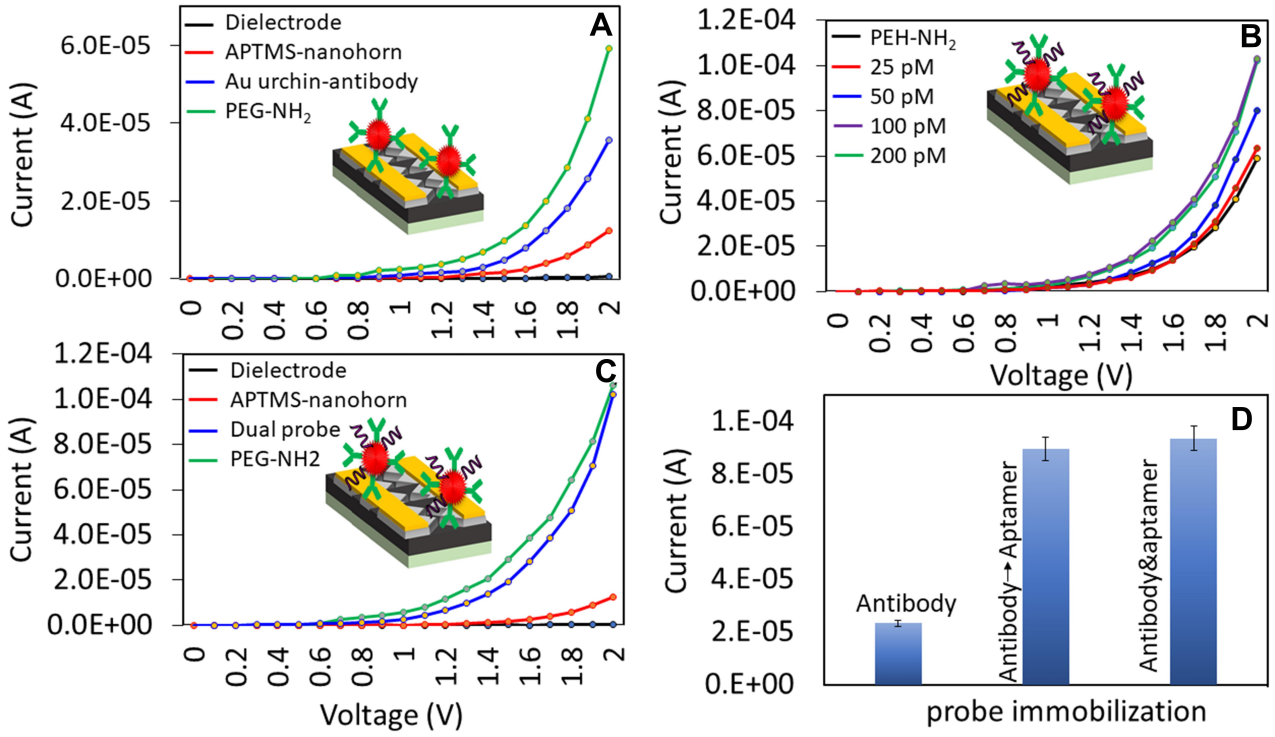

Figure 4 Comparison of probe immobilization on nanohorn-modified electrodes. (**A**) Au urchin antibody immobilization on APTMS-nanohorn; (**B**) aptamer titration on Au-urchin-antibody attached electrode; (**C**) dual probe of antibody-aptamer immobilization on APTMS-nanohorn; Figure insets are diagrammatic. (**D**) Comparison of current changes with different probe immobilizations. The dual probe of the aptamer and antibody shows the highest current response.

In the second case (method 2), Au antibody was attached as explained previously, and then aptamer was added until the surface was saturated. Thiolated aptamers can attach to the excess surface area of Au urchins. Since the antibody is large, it automatically forms gaps between antibodies when attached to the surface of the Au urchin. Our idea was to fill the gaps with the smaller sized aptamer. As shown in Figure 4B, when 25 pM aptamer was added, little current was noted (brown line). Increasing the concentration to 50 pM changed the current from 1.02 E-04 to 8.01 E-05 A. This result confirmed the binding of the aptamer on the surface of the Au-urchin. Furthermore, upon increasing the aptamer concentration to 100 and 200 pM, clear current changes were noted. It was further noticed that aptamer binding was saturated at 200 pM. This antibody-aptamer-modified surface was used to compare the detection of AβO with those by other methods.

In the last method (method 3), an aptamer was attached to the surface of the Au urchin antibody. After attaching the antibody to the Au urchin, 200 pM aptamer was added to cover the excess surface. This helped to reduce the steps and time of the probe immobilization process, and the aptamer could attach more readily to the Au urchin surface in solution than to the surface. Figure 4C displays a dual probe with an antibody aptamer on a Au urchin immobilized on a nanohorn-modified electrode surface. After attaching the APTMS nanohorn (red line), the dual probe was directly added, and the observed current increased from 1.24 E-05 to 1.06 E-04 A. This increase in current confirmed the binding of the probe on the sensing electrode surface. Compared to the previous method of probe immobilization, the antibody probe showed a current difference of 2.34 E-05 A, the antibody followed by aptamer immobilization showed a current difference of 8.96 E-05 A, and with the antibody-aptamer as a dual probe, the current difference was 9.36E-05 A (Figure 4D). It was clearly concluded that when aptamer was added with antibody, the current level increased approximately 4 times more that with the case of antibody alone. It was also noted that there was little difference between method 2 (antibody and then aptamer) and method 3 (dual probe of aptamer and antibody). From this result, it was concluded that the dual probe method is an efficient immobilization method for attaching both aptamers and antibodies simultaneously on sensing surfaces. This probing system also

possibly interacts with a higher number of AβOs and enhances detection.

Comparative Detection of AβO on Different Probe Immobilized Electrode Surfaces

Detection of AβO at a 1 nM concentration was compared for three different probe-immobilized electrode surfaces (methods 1, 2 and 3). AβO was dripped onto the probe-attached surface, and the current changes were noted. On the antibody-modified surface, 1 nM AβO was added and the current response changed from 3.57 E-05 to 5.68 E-06 A (Figure 5A). A similar amount of 1 nM AβO was added to the antibody- and aptamer-modified surfaces, and the current changed from 1.06 E-04 to 7.22 E-06 A (Figure 5B). Finally, the current was changed from 1.02 E-04 to 3.98 E-07 A when AβO was dripped onto the dual probe of the aptamer and antibody-modified surface (Figure 5C). The differences in currents noted for 1 nM AβO detection were 2.9 E-06 A in method 1, 9.878 E-06 in method 2 and 10.1 E-06 A in method 3 (Figure 5D). This result indicated that the dual probe increased the current flow with the same concentration of AβO (1 nM) due to the binding of AβO with the aptamer and antibody.

Limit of Detection of AβO: A Linear Regression Analysis

To calculate the limit of AβO detection, different dilutions of AβO (0.01 to 100 pM) were individually dripped onto probe-modified surfaces. Figure 6A shows the current changes observed after dripping AβO on antibody-aptamer-modified surfaces (method 2). Upon adding 10 fM AβO, the current was changed from 1.06E-04 to 2.8 E-05 A. This result shows the interaction of 0.01 pM AβO with the antibody and aptamer. With further increases in the concentrations of AβO to 0.1, 1, 10, and 100 pM, the current flows gradually decreased to 1.64E-05, 1.33 E-05, 8.85E-06 and 7.34 E-06 A, respectively. It was noticed that concentrations of 10 and 100 pM showed saturation in the current changes.

A similar experiment was conducted on an aptamer-antibody dual probe immobilized electrode surface (method 3) (Figure 6B). In this case, after adding 10 fM AβO, the current was changed from 1.02E-04 to 2.35 E-05 A. This result confirmed the interaction of 0.01 pM of AβO with the antibody and aptamer. With further increases in the concentrations of AβO to 0.1, 1, 10, and 100 pM, the current flows gradually decreased to 1.59E-05, 1.15 E-05, 5.03E-06 and 2.97 E-06 A, respectively. When comparing these two

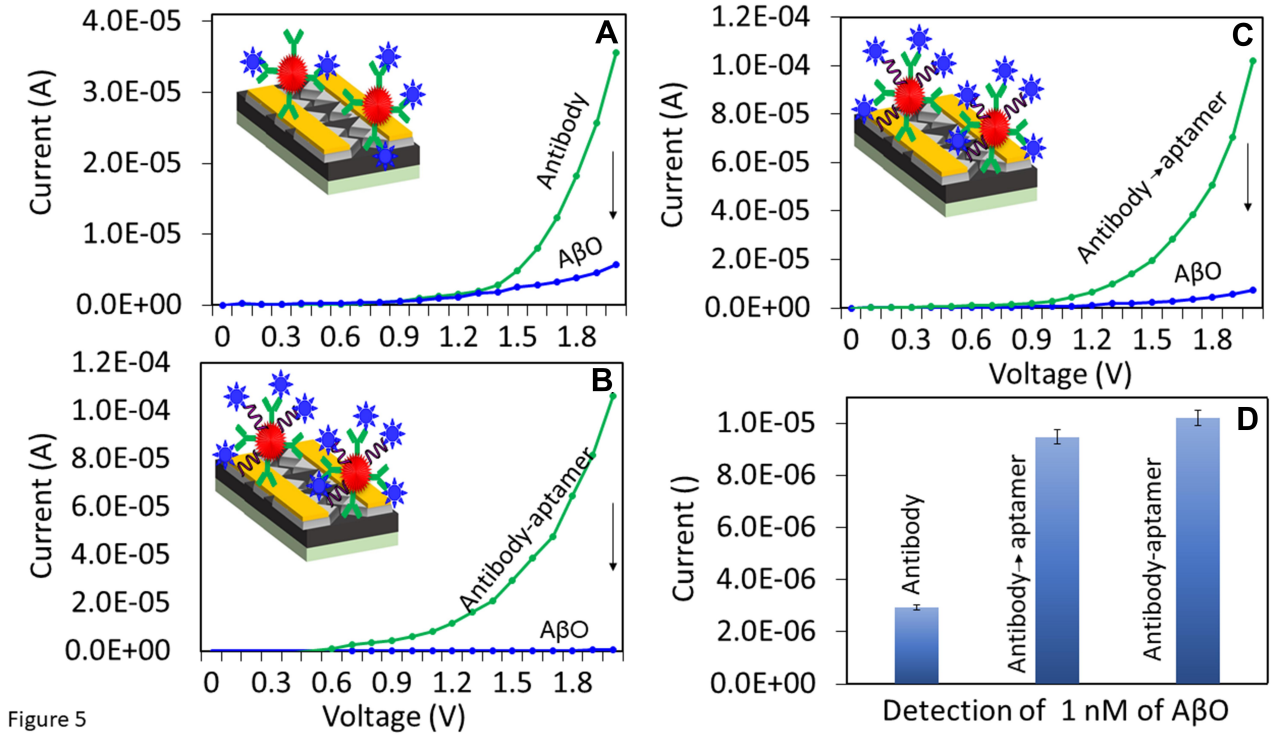

Figure 5

Figure 5 Comparison of detection of 1 nM AβO on (**A**) Au urchin antibody immobilized electrode; (**B**) antibody-aptamer immobilized electrode; (**C**) dual probe of antibody-aptamer immobilized electrode; Figure insets are diagrammatic. (**D**) Comparison of current changes of AβO detection with different probes. A dual probe with an aptamer and antibody shows the highest current response.

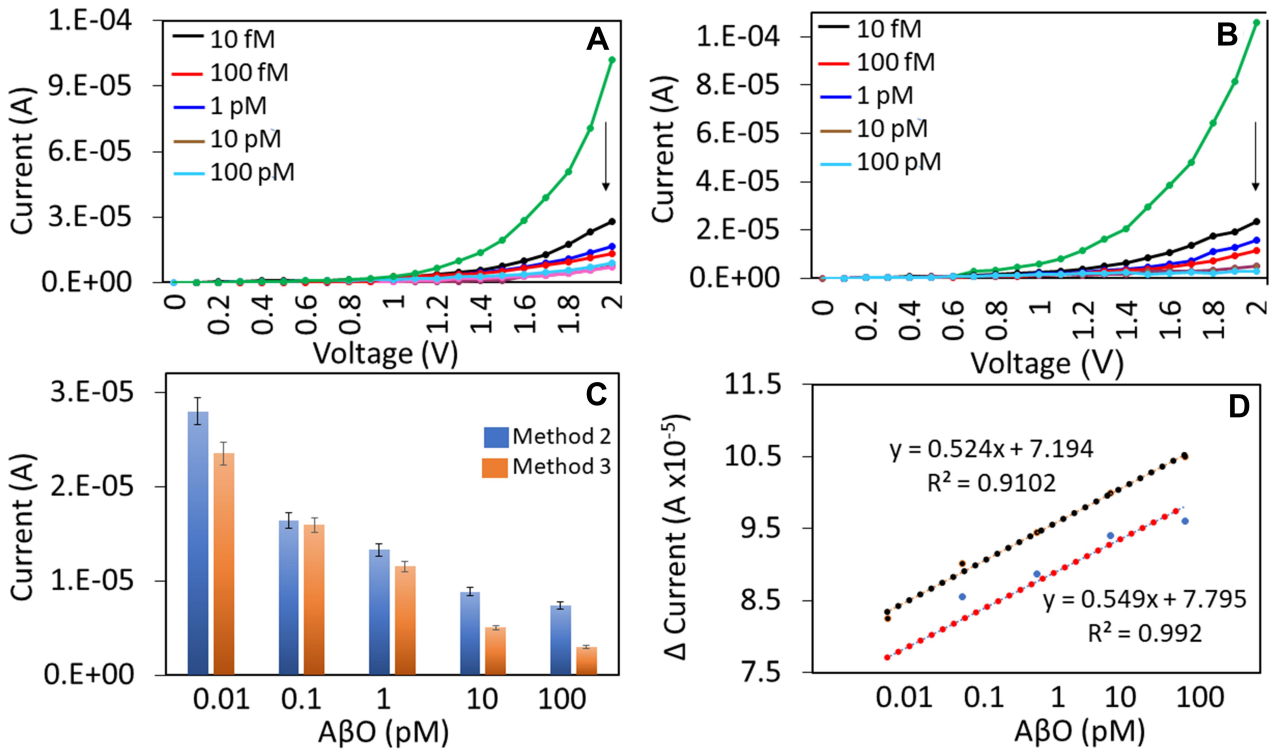

Figure 6 Different concentrations of AβO by titration (0.01–100 pM) on (**A**) Antibody-aptamer immobilized electrode; (**B**) dual probe of antibody-aptamer immobilized electrode; (**C**) comparison of current changes with AβO titration, dual probe shows the highest current response with all AβO concentrations; (**D**) difference in current changes in AβO determination were plotted in an Excel sheet and used to calculate the detection limit. The detection limit was found to be 10 fM by both methods.

detection methods for AβO identification, method 3 shows a higher current response than method 2. Furthermore, the saturation point was 100 pM with the dual probe, while it was 10 pM with the antibody-aptamer probe surface (Figure 6C). These results indicated that the dual probe method attracted a higher number of AβOs and increased the current responses. The current difference was calculated for each AβO concentration (in methods 2 and 3) and plotted in an Excel sheet to calculate the limit of detection. As shown in Figure 6D, both methods showed the same detection limit of

Table 1 Comparing Detection of Aβ with Available Methods

Sensor	Target	Probe	Detection limit	Linear range	Reference
Smart near infrared fluorescence	Aβ 1-42	π-electron chain for Aβ -plaques	0.027 μM	-	(33)
EIS sensor	Aβ-40	Aptamer	~20 fM	0.1 pg/mL-10 μg/mL	(34)
Electrochemical sensor	Aβ 1-42	Aptamer	$3.5x10^{-14}$ mol/L	$1x10^{-13}$ to $1x10^{-8}$ mol/L	(35)
Electrochemical sensor	AβO	Aptamer-antibody	100 pM	0.5-30 nM	(8)
Impedance sesnor	AβO	Cellular prion protein	0.1 pM	10^{-8} to 10^{4} nM	(36)
Amperometric sensor	Aβ	Aptamer	0.002 pM	0.1 pM-10 nM	(37)
SERS	Aβ	Sialic acid	1 pM	1 pM-11.5 nM	(38)
Colorimetric assay	AβO	PrP	20 nM	20-100 nM	(39)
Fluorescent sensor	Aβ	CRANAD-2	38 nM	-	(40)
Electrochemical sensor	AβO	Aptamer-antibody	10 fM	0.01-100 pM	This work

Abbreviations: EIS, electrode-insulator-semiconductor sensor; FET, field effect transistor.

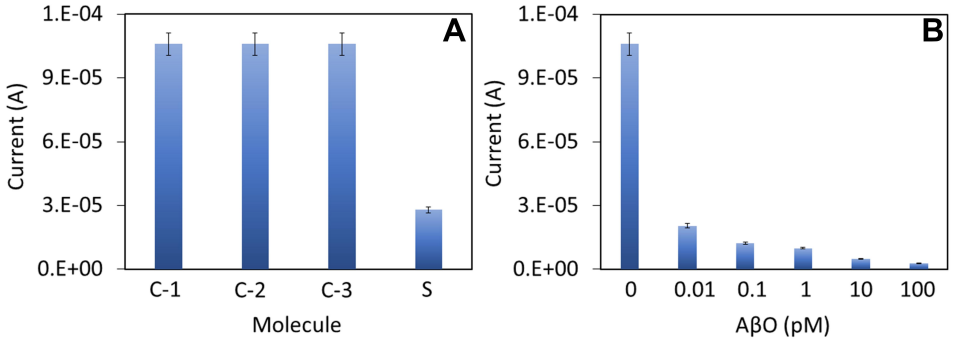

Figure 7 Selective detection. (**A**) AβO was identified with C-1 (no AβO), C-2 (with nonimmune and complementary aptamers), and C-3 (with control protein). No significant changes were noted in any of the above three control experiments compared with the specific interaction(s) of AβO with its antibody and aptamer. (**B**) Spiking experiment. Different AβO concentrations (0.01, 0.1, 1 and 10 pM) in artificial CSF were dripped independently on dual probe-modified surfaces. CSF did not interfere with the interaction of AβO with its antibody and aptamer.

0.01 pM (10 fM), but the dual probe showed higher changes in current with all AβO concentrations. This attainment attested to the good sensitivity of the sensor and was comparable to the current sensors used for determining AD (Table 1).

Selectivity, Reproducibility and Stability for AβO Determination: High-Performance Analysis

Specific identification of AβO was monitored with three different control experiments, which included experiments without AβO, with nonimmune antibody and complementary aptamer sequences, and with α-synuclein instead of AβO. These three control experiments did not give significant current responses, which confirmed specific AβO detection (Figure 7A).

To mimic AβO detection in real-life situations, different AβO concentrations (0.01, 0.1, 1, 10, and 100 pM) were spiked into artificial CSF and dripped onto dual probe-modified surfaces for interaction. As shown in the figure, clear changes in the current response were noted with different AβO concentrations spiked into CSF. There was no significant current response compared with the detection of AβO in the presence or absence of CSF (Figure 7B). This means that AβO was specifically recognized by the aptamer and antibody on the immobilized electrode surfaces. Reproducibility is mandatory confirmation in any sensor and is needed to obtain accurate results for high-performance target identification. Here, current responses with five different electrodes were monitored, including surfaces modified with APTMS nanohorns, dual antibody-aptamer probes, PEH-NH_2 and AβO.

Conclusion

This research involved studies of the Alzheimer's disease biomarker amyloid-beta oligomer (AβO) on a nanohorn-modified electrode surface. A nanohorn was attached to the electrode surface through an amine linker, and then a dual probe of aptamer-antibody-modified Au urchin was attached to the nanohorn. This dual probe-modified surface improved the detection of AβO, and the current flow was compared with that seen with only antibody as the probe; the improved system realized a detection limit of 10 fM. Since the dual probe interacted with a higher number of AβOs, enhanced current changes were noticed at all AβO concentrations used. Furthermore, control experiments failed to change the current flow, confirming the specific detection of AβO. In addition, spiking AβO into the artificial CSF did not interfere with the detection of AβO, indicating the selective determination of AβO. This dual probe-modified electrode surface helps to identify AβO and diagnose Alzheimer's disease.

Acknowledgment

SCBG was supported by a special grant (9001-00596) from Universiti Malaysia Perlis.

Disclosure

The authors report no conflicts of interest for this work.

References

1. Sun LP, Zhong Y, Gui J, Wang XW, Zhuang XR, Weng J. A hydrogel biosensor for high selective and sensitive detection of amyloid-beta oligomers. *Int J Nanomedicine*. 2018;13:843–856. doi:10.2147/IJN.S152163

2. Pundir CS, Narwal V. Biosensing methods for determination of triglycerides: a review. *Biosens Bioelectron*. 2018;100:214–227. doi:10.1016/j.bios.2017.09.008
3. Bae JB, Lee S, Jung W, et al. Identification of Alzheimer's disease using a convolutional neural network model based on T1-weighted magnetic resonance imaging. *Sci Rep*. 2020;10(1):1–10. doi:10.1038/s41598-020-79243-9
4. Azimzadeh M, Nasirizadeh N, Rahaie M, Naderi-Manesh H. Early detection of Alzheimer's disease using a biosensor based on electrochemically-reduced graphene oxide and gold nanowires for the quantification of serum microRNA-137. *RSC Adv*. 2017;7(88):55709–55719. doi:10.1039/C7RA09767K
5. Arslan J, Jamshed H, Qureshi H. Early Detection and Prevention of Alzheimer's Disease: role of Oxidative Markers and Natural Antioxidants. *Front Aging Neurosci*. 2020;12:1–7. doi:10.3389/fnagi.2020.00231
6. Toyos-Rodríguez C, García-Alonso FJ, de la Escosura-Muñiz A. Electrochemical biosensors based on nanomaterials for early detection of alzheimer's disease. *Sensors (Switzerland)*. 2020;20(17):1–43. doi:10.3390/s20174748
7. Liu D, Fu D, Zhang L, Sun L. Detection of amyloid-beta by Fmoc-KLVFF self-assembled fluorescent nanoparticles for Alzheimer's disease diagnosis. *Chin Chem Lett*. 2020;2019. doi:10.1016/j.cclet.2020.09.009.
8. Zhou Y, Zhang H, Liu L, et al. Fabrication of an antibody-aptamer sandwich assay for electrochemical evaluation of levels of β-amyloid oligomers. *Sci Rep*. 2016;6:1–8. doi:10.1038/s41598-016-0001-8
9. Sun L, Liu D, Fu D, Yue T, Scharre D, Zhang L. Fluorescent peptide nanoparticles to detect amyloid-beta aggregation in cerebrospinal fluid and serum for Alzheimer's disease diagnosis and progression monitoring. *Chem Eng J*. 2021;405:126733. doi:10.1016/j.cej.2020.126733
10. Veloso AJ, Chow AM, Ganesh HVS, et al. Electrochemical immunosensors for effective evaluation of amyloid-beta modulators on oligomeric and fibrillar aggregation processes. *Anal Chem*. 2014;86(10):4901–4909. doi:10.1021/ac500424t
11. Yi X, Feng C, Hu S, Li H, Wang J. Surface plasmon resonance biosensors for simultaneous monitoring of amyloid-beta oligomers and fibrils and screening of select modulators. *Analyst*. 2016;141:331–336. doi:10.1039/C5AN01864A
12. Wennmalm S, Chmyrov V, Widengren J, Tjernberg L. Highly Sensitive FRET-FCS Detects Amyloid β-Peptide Oligomers in Solution at Physiological Concentrations. *Anal Chem*. 2015;87(23):11700–11705. doi:10.1021/acs.analchem.5b02630
13. Zhao J, Chang W, Liu L, et al. Graphene oxide-gold nanoparticle-aptamer complexed probe for detecting amyloid beta oligomer by ELISA-based immunoassay. *J Immunol Methods*. 2021;489:112942. doi:10.1016/j.jim.2020.112942
14. Liu F, Zhang J, Chen R, Chen L, Deng L. Highly effective colorimetric and visual detection of ATP by a DNAzyme-aptamer sensor. *Chem Biodivers*. 2011;8(2):311–316. doi:10.1002/cbdv.201000130
15. Gopinath SCB, Sakamaki Y, Kawasaki K, Kumar PKR. An Efficient RNA Aptamer against Human Influenza B Virus Hemagglutinin. *J Biochem*. 2006;139(5):837–846. doi:10.1093/jb/mvj095
16. Gopinath SCB, Misono TS, Kumar PKR. Prospects of Ligand-Induced Aptamers. *Crit Rev Anal Chem*. 2008;38(1):34–47. doi:10.1080/10408340701804558
17. Gopinath SCB, Shikamoto Y, Mizuno H, Kumar P. A Potent Anti-Coagulant RNA Aptamer Inhibits Blood Coagulation by Specifically Blocking the Extrinsic Clotting Pathway. *Thromb Haemost*. 2006;95:767–771. doi:10.1160/TH06-01-0047
18. Lakshmipriya T, Fujimaki M, Gopinath SCB, Awazu K. Generation of anti-influenza aptamers using the systematic evolution of ligands by exponential enrichment for sensing applications. *Langmuir*. 2013;29(48):15107–15115. doi:10.1021/la4027283
19. Gopinath SCB, Lakshmipriya T, Awazu K. Colorimetric detection of controlled assembly and disassembly of aptamers on unmodified gold nanoparticles. *Biosens Bioelectron*. 2014;51:115–123. doi:10.1016/j.bios.2013.07.037
20. Lakshmipriya T, Horiguchi Y, Nagasaki Y. Co-immobilized poly(ethylene glycol)-block-polyamines promote sensitivity and restrict biofouling on gold sensor surface for detecting factor IX in human plasma. *Analyst*. 2014;139(16):3977–3985. doi:10.1039/C4AN00168K
21. Jarczewska M, Malinowska E. The application of antibody-aptamer hybrid biosensors in clinical diagnostics and environmental analysis. *Anal Methods*. 2020;12(25):3183–3199. doi:10.1039/D0AY00678E
22. Serban B-C, Bumbac M, Buiu O, Cobianu C, Brezeanu M, Nicolescu C. Carbon Nanohorns and Their Nanocomposites: synthesis, Properties and Applications. a Concise Review. *Ann Acad Rom Sci Ser Sci Technol Inf*. 2018;11(2):5.
23. Zhu S, Xu G. Single-walled carbon nanohorns and their applications. *Nanoscale*. 2010;2(12):2538–2549. doi:10.1039/c0nr00387e
24. Zhu G, Sun H, Zou B, et al. Electrochemical sensing of 4-nitrochlorobenzene based on carbon nanohorns/graphene oxide nanohybrids. *Biosens Bioelectron*. 2018;106:136–141. doi:10.1016/j.bios.2018.01.058
25. Zhu G, Fiston MN, Qian J, Kingsford OJ. Highly sensitive electrochemical sensing of: para -chloronitrobenzene using a carbon nanohorn-nanotube hybrid modified electrode. *Anal Methods*. 2019;11:1125–1130. doi:10.1039/C8AY02680G
26. Tsukakoshi K, Abe K, Sode K, Ikebukuro K. Selection of DNA aptamers that recognize α-synuclein oligomers using a competitive screening method. *Anal Chem*. 2012;84(13):5542–5547. doi:10.1021/ac300330g
27. Liu L, He Q, Zhao F, et al. Competitive electrochemical immunoassay for detection of β-amyloid (1-42) and total β-amyloid peptides using p-aminophenol redox cycling. *Biosens Bioelectron*. 2014;51:208–212. doi:10.1016/j.bios.2013.07.047
28. Hegnerová K, Bocková M, Vaisocherová H, et al. Surface plasmon resonance biosensors for detection of Alzheimer disease biomarker. *Sens Actuators B Chem*. 2009;139:69–73. doi:10.1016/j.snb.2008.09.006
29. Ramanathan S, Gopinath SCB, Arshad MKM, et al. Aluminosilicate Nanocomposite on Genosensor: a Prospective Voltammetry Platform for Epidermal Growth Factor Receptor Mutant Analysis in Non-small Cell Lung Cancer. *Sci Rep*. 2019. doi:10.1038/s41598-019-53573-9
30. Letchumanan I, Gopinath SCB, Md arshad MK, Anbu P, Lakshmipriya T. Gold nano-urchin integrated label-free amperometric aptasensing human blood clotting factor IX: a prognosticative approach for "Royal disease.". *Biosens Bioelectron*. 2019;131:128–135. doi:10.1016/j.bios.2019.02.006
31. Lakshmipriya T, Fujimaki M, Gopinath SCB, Awazu K, Horiguchi Y, Nagasaki Y. A high-performance waveguide-mode biosensor for detection of factor IX using PEG-based blocking agents to suppress non-specific binding and improve sensitivity. *Analyst*. 2013;138(10):2863. doi:10.1039/c3an00298e
32. Nagasaki Y. Construction of a densely poly(ethylene glycol)-chain-tethered surface and its performance. *Polym J*. 2011;43(12):949–958. doi:10.1038/pj.2011.93
33. Cui M,Ono M,Watanabe H,Kimura H,Liu B,Saji H. Smart near-infrared fluorescence probes with donor-acceptor structure for in vivo detection of β-amyloid deposits. *J Am Chem Soc*. 2014;136(9):3388–94.
34. Kutovyi Y, Hlukhova H, Boichuk N, Menger M, Offenhäusser A, Vitusevich S. Amyloid-beta peptide detection via aptamer-functionalized nanowire sensors exploiting single-trap phenomena. *Biosens Bioelectron*. 2020;154(November 2019).

35. Qin H, Gao X, Yang X, Cao W, Liu S. A label-free and signal-on electrochemiluminescence strategy for sensitive amyloid-beta assay. *Biosens Bioelectron*. 2019;141:111438.
36. Qin J, Cho M, Lee Y. Ultrasensitive Detection of Amyloid-β Using Cellular Prion Protein on the Highly Conductive Au Nanoparticles-Poly(3,4-ethylene dioxythiophene)-Poly(thiophene-3-acetic acid) Composite Electrode. *Anal Chem*. 2019;91(17):11259–65.
37. Zhang Y, Figueroa-Miranda G, Zafiu C, Willbold D, Offenhäusser A, Mayer D. Amperometric Aptasensor for Amyloid-β Oligomer Detection by Optimized Stem-Loop Structures with an Adjustable Detection Range. *ACS Sensors*. 2019;4(11):3042–50.
38. Chou IH, Benford M, Beier HT, Cotè GL, Wang M, Jing N, et al. Nanofluidic biosensing for β-amyloid detection using surface enhanced raman spectroscopy. *Nano Lett*. 2008;8(6):1729–35.
39. Xia N, Zhou B, Huang N, Jiang M, Zhang J, Liu L. Visual and fluorescent assays for selective detection of beta-amyloid oligomers based on the inner filter effect of gold nanoparticles on the fluorescence of CdTe quantum dots. *Biosens Bioelectron*. 2016;85:625–32.
40. Chongzhao R, Xiaoyin X, Raymond SB, Ferrara BJ, Neal K, Bacskai BJ, et al. Design, synthesis, and testing of difluoroboron-derivatized curcumins as near-infrared probes for in vivo detection of amyloid-β deposits. *J Am Chem Soc*. 2009;131(42):15257–61.